140 *Macromolecules* **2011**, *44*, 140–146
DOI: 10.1021/ma102154u

Macromolecules
ARTICLE

Universality in Nonlinear Elasticity of Biological and Polymeric Networks and Gels

Andrey V. Dobrynin* and Jan-Michael Y. Carrillo

Polymer Program, Institute of Materials Science and Department of Physics, University of Connecticut, Storrs, Connecticut 06269, United States

Received September 16, 2010; Revised Manuscript Received November 18, 2010

ABSTRACT: Networks and gels are part of our everyday experience starting from automotive tires and rubber bands to biological tissues and cells. Biological and polymeric networks show remarkably high deformability at relatively small stresses and can sustain reversible deformations up to 10 times their initial size. A distinctive feature of these materials is highly nonlinear stress−strain curves leading to material hardening with increasing deformation. This differentiates networks and gels from conventional materials, such as metals and glasses, showing linear stress−strain relationship in the reversible deformation regime. Using theoretical analysis and molecular dynamics simulations, we propose and test a theory that describes nonlinear mechanical properties of a broad variety of biological and polymeric networks and gels by relating their macroscopic strain-hardening behavior with molecular parameters of the network strands. This theory provides a universal relationship between the strain-dependent network modulus and the network deformation and explains strain-hardening of natural rubber, synthetic polymeric networks, and biopolymer networks of actin, collagen, fibrin, vimentin, and neurofilaments.

The characteristic feature of biological and polymeric networks and gels is the predominantly entropic nature of their elasticity.[1] The elastic response of these materials is due to extension of the individual chains or filaments reducing the number of available molecular conformations and hence the configurational entropy of the system. The entropic nature of the network elasticity allows large reversible deformations. In Figure 1, we combined stress−strain curves for natural rubber,[1,2] synthetic polymeric networks,[2,3] and biopolymer networks[4] of actin, collagen, fibrin, vimentin, and neurofilaments. The natural rubber[1,2] and synthetic networks[2,3] are dense polymeric systems consisting of highly coiled polymeric chains. The typical stress necessary for network deformations is on the order of 10^4-10^7 Pa. These networks can recover their initial form after up to a 10-fold increase in their original size, $\varepsilon \propto 10$. The biological networks are sparse and filled with water such that the filaments making up the network are only slightly coiled.[4] The deformation of these networks requires significantly low stresses ($10^{-1}-10^2$ Pa) and they can reversibly deform under the shear strain, $\gamma \leq 10$.[4] The striking similarity between two different classes of the network materials is the stress-induced network hardening which is manifested in the highly nonlinear stress−strain deformation curves (see Figure 1).

Modern theories of elasticity of networks and gels are based on the elastic response of the individual network strands making up the network.[1,5] These theories treat polymeric and biological networks as two different classes of systems. The deformation of strands of polymeric networks is usually described by the freely jointed chain model.[1,5] The deformation of biological networks made of stiff biological macromolecules or filaments[4,6−10] is modeled by the worm-like chain model.[6,11−14] In the small deformation limit both models give linear relationship between the magnitude of the local tension and the strand deformation.[5] But for the large strand deformations that correspond to the nonlinear network deformation regime, two models demonstrate qualitatively different divergence of the local tension f as a size of the deformed network strand R approaches its maximum value R_{max}. For the freely jointed chain model the local tension diverges as, $f \propto (R_{max} - R)^{-1}$, while for the worm-like chain model the tension f exhibits a faster divergence $f \propto (R_{max} - R)^{-2}$.[5] This results in a qualitatively different strain-hardening behavior of polymeric and biological networks and gels.

However, it was shown recently that polymer chains behave as a worm-like chain under tension in the interval of the applied forces f smaller than the crossover force f_c and as a freely jointed chain for $f > f_c$.[15−18] Magnitude of the crossover force $f_c \propto Kk_BT/b$ depends on the effective chain bending constant K (or chain persistence length l_p) and bond length b (k_B is the Boltzmann constant and T is the absolute temperature). For biological macromolecules like DNA the crossover force is estimated to be on the order of 4 nN while for flexible chains such as polystyrene, single stranded DNA, and PDMS it is on the order of 20−300 pN.[15,18] Universality in single chain deformation behavior indicates that one should expect universality in elastic properties of polymeric and biological networks and gels in the range of strains for which the forces acting on the network strands are smaller than a crossover force. Below we will show that this universality exists. To prove this we use a nonlinear deformation model of a worm-like chain[19] and derive expressions for the network stress under uniaxial and shear deformations. The derivation details are worked out in the Appendix A.

In the case of the uniaxial deformation at a constant volume the network extends in one direction say along the x-axis $\lambda_x = \lambda$ while it contracts in two others

$$\lambda_y = \lambda_z = 1/\sqrt{\lambda}$$

(see Figure 2).[1,5] The true stress generated in the uniaxially deformed network is equal to

$$\sigma_{xx}(\lambda) = \frac{G}{3}(\lambda^2 - \lambda^{-1})\left(1 + 2\left(1 - \frac{\beta I_1(\lambda)}{3}\right)^{-2}\right) \qquad (1)$$

*Corresponding author.

 Published on Web 12/09/2010

where the first strain invariant for the uniaxial deformation is $I_1(\lambda) = (\lambda^2 + 2/\lambda)$. Thus, the magnitude of the network stress depends on two parameters: the network shear modulus G and the chain elongation ratio β. The network shear modulus $G \approx k_B T\rho\langle R_{in}^2\rangle/\langle R_0^2\rangle N_s$ depends on the monomer density ρ, the average number of bonds N_s between cross-links, and the intrinsic chain extension $\langle R_{in}^2\rangle/\langle R_0^2\rangle$—the ratio of the mean-square average end-to-end distance of the strand in the undeformed network $\langle R_{in}^2\rangle$ to its ideal value $\langle R_0^2\rangle$. Note that in the case of the natural rubber $\langle R_{in}^2\rangle = \langle R_0^2\rangle$. The second molecular parameter describing network properties is $\beta = \langle R_{in}^2\rangle/R_{\max}^2$ which is the ratio of $\langle R_{in}^2\rangle$ and the square of the end-to-end distance of the fully extended strand $R_{\max}^2$.

For a shear deformation a shear strain γ is equal to $\gamma = \tan\phi$ (see Figure 2).[1] The shear stress can be written as follows

$$\sigma_{xy}(\gamma) = \frac{G\gamma}{3}\left(1 + 2\left(1 - \frac{\beta I_1(\gamma)}{3}\right)^{-2}\right) \qquad (2)$$

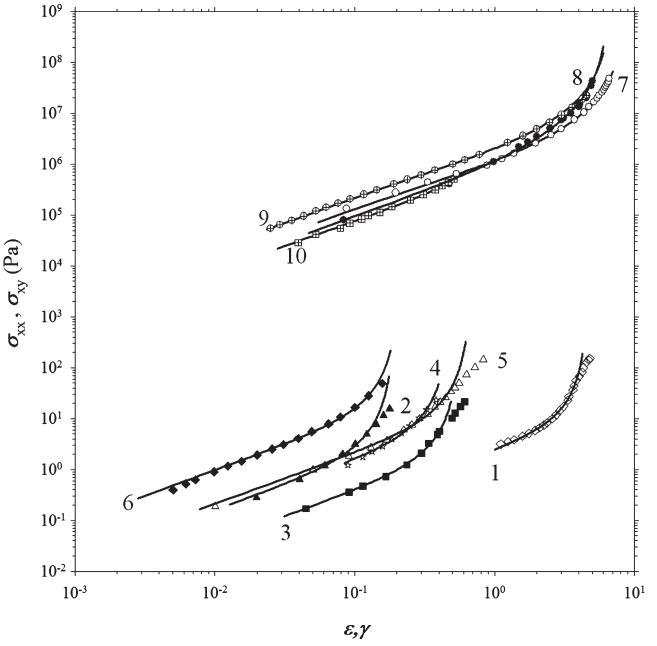

Figure 1. Stress−strain deformation curves of neurofilament network (1), collagen network (2), vimentin network (3), fibrin network (4, 5), actin network (6), natural rubber (7−9), and PPG BisAcAc−EA−HMDI−EA network (10). For natural rubber (7−9) and polymeric network (10) we have converted the original data sets for the engineering stress to the true stress $\sigma_{xx} = (1 + \varepsilon)\sigma_{xx}^{eng}$. The lines represent a best fit to the theoretical expression for stress−strain deformation curve (see text for details).

where the first strain invariant for the shear deformation is given by $I_1(\gamma) = \gamma^2 + 3$.

The diverging term appearing in eqs 1 and 2 reflects finite extensibility of the strands between cross-links. It has the same quadratic divergence as the singular term in the expression for tension in a stretched worm-like chain (see Appendix A).

We have applied eqs 1 and 2 to fit the stress−strain curves for networks shown in Figure 1. For uniaxial deformation the elongation strain $\varepsilon = \lambda - 1$. The lines in Figure 1 correspond to the best fits to eqs 1 and 2. Note that for the weakly cross-linked networks at small deformations the part of the stress is supported by entanglements. To account for the entanglement contributions we have added a Mooney−Rivlin term[1,5] to the chain's free energy and to the network stress (see Appendix B). From fitting experimental data sets to eqs 1 and 2, we have obtained values of the network shear modulus G and the chain elongation ratio β. These parameters are summarized in Table 1. The data presented in Table 1 show that polymeric networks have a shear modulus G on the order of MPa and chain elongation ratios $\beta \propto 10^{-2}$−0.4. The small values of the chain elongation ratio support the idea that in polymeric networks the network strands are coiled. On the contrary, the chain elongation ratios for biological networks are close to unity indicating that filaments forming these networks are almost fully extended due to high values of the filament bending modulus and persistence length. Furthermore, the typical values of the shear modulus for biological networks are on the order of $G \propto 10^{-2}$−1 Pa with the largest value of the shear modulus corresponding to a network of the neurofilaments and the smallest value obtained for a collagen network. The network shear modulus decreases with increasing the filament rigidity, $G \propto k_B T\rho b/l_p$, which immediately follows from dependence of the network shear modules G on the system parameters $\langle R_{in}^2\rangle \approx R_{\max}^2 \approx b^2 N_s^2$ (for $\beta \approx 1$), and $\langle R_0^2\rangle \approx 2 l_p R_{\max}$.

To test predictions of our theory, we have performed molecular dynamics simulations[21] of the coarse-grained model of randomly cross-linked networks. The simulations details are described in Appendix C. We have performed simulations of the networks undergoing uniaxial and shear deformations. Figure 3 presents simulation results for uniaxial deformation of networks consisting of polymeric strands with different values of the chain bending constant. The lines correspond to the best fit to eq 1 considering shear modulus G and elongation ratio β as adjustable parameters. The values of the fitting parameters are given in Table 1. Note that the values of the chain elongation ratios obtained from the fitting procedure are close to the one directly calculated from the structures of the undeformed networks (see Appendix C). As one can see from this plot the agreement between simulation results and theoretical expression for uniaxial network deformation eq 1 is excellent. It is interesting to point out that the simulations also show a decrease in network shear modulus with increasing strand stiffness (persistence length) (see Appendix C).

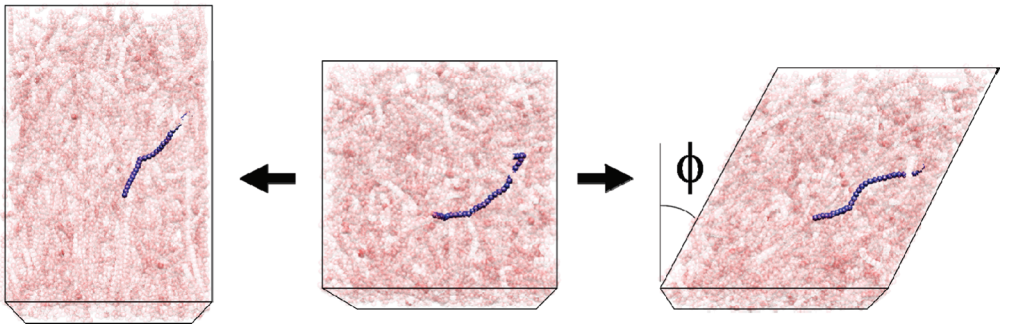

Figure 2. Snapshots of the simulation box of the network deformation at a constant volume. Uniaxial deformation (left) and shear (right).

Table 1. Network Parameters: Shear Modulus G, Chain Elongation Ratio β and Ratio of the Shear Modulus Due to Entanglements G_e to the Shear Modulus G, G_e/G

		experiments		
	system	G	β	G_e/G
1	neurofilaments[4]	1.9283 Pa	0.1182	--
2	collagen[4]	0.0039 Pa	0.9873	--
3	vimentin[4]	0.0582 Pa	0.8988	--
4	fibrin (steady state)[4]	0.1275 Pa	0.9246	--
5	fibrin (oscillatory)[4]	0.5982 Pa	0.8619	--
6	actin[4]	0.0319 Pa	0.9852	--
7	natural rubber[1]	0.198 MPa	0.0294	1.25
8	natural rubber[20]	0.294 MPa	0.0477	--
9	natural rubber[2]	0.356 MPa	0.0438	1.06
10	PPG BisAcAc−EA−HMDI−EA network[3]	0.1084 MPa	0.4056	--
11	PPG BisAcAc−NPGDA network[3]	0.0399 MPa	0.042	0.71
12	SBR[2]	0.187 MPa	0.0255	2.41

		Simulations		
	system	$G \times 10^3[k_BT/\sigma^3]$	β	G_e/G
13	$K = 2$, $N_s = 17.88 \pm 7.4$, uniaxial deformation	7.40	0.198	--
14	$K = 5$, $N_s = 18.03 \pm 6.7$, uniaxial deformation	4.73	0.45	--
15	$K = 10$, $N_s = 17.90 \pm 6.7$, uniaxial deformation	3.04	0.633	--
16	$K = 10$, $N_s = 17.90 \pm 6.7$, shear deformation	3.04	0.654	--
17	$K = 20$, $N_s = 17.98 \pm 6.7$, uniaxial deformation	2.27	0.752	--
18	$K = 20$, $N_s = 17.98 \pm 6.7$, shear deformation	2.27	0.742	--
19	$K = 30$, $N_s = 17.83 \pm 6.6$, uniaxial deformation	2.15	0.791	--
20	$K = 40$, $N_s = 17.99 \pm 6.7$, uniaxial deformation	1.30	0.806	--
21	$K = 40$, $N_s = 17.99 \pm 6.7$, shear deformation	1.30	0.808	--

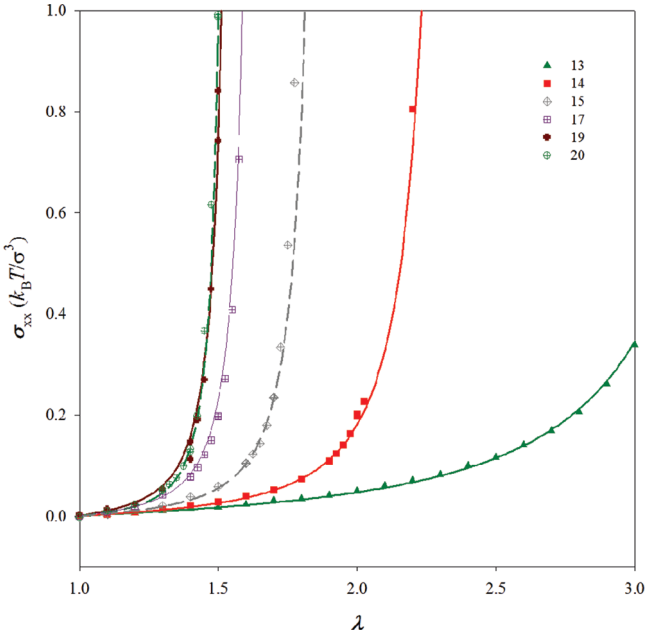

Figure 3. Dependence of the true stress σ_{xx} on the deformation ratio λ for uniaxially deformed networks. Numbers correspond to the networks described in Table 1.

Using eqs 1 and 2 we can introduce a deformation dependent network shear modulus in the case of the uniaxial and shear deformations as

$$G(I_1) \equiv \frac{\sigma_{xx}(\lambda)}{\lambda^2 - \lambda^{-1}} = \frac{G}{3}\left(1 + 2\left(1 - \frac{\beta I_1(\lambda)}{3}\right)^{-2}\right) \qquad (3a)$$

and

$$G(I_1) \equiv \sigma_{xy}(\gamma)/\gamma \qquad (3b)$$

Equations 3a and 3b are the main results of the paper. They are different from the previous theoretical results on nonlinear network elasticity.[1,4,6−10] For the first time, we have been able to derive the invariant expression for the strain-dependent network shear modulus. This modulus is a universal function of the strain invariant I_1 characterizing network deformation and parameter β determining the stretching ability of the strands between cross-links. Thus, biological and polymeric networks and gels should demonstrate similar nonlinear behavior, because molecular specificity of strands forming networks or gels enters the problem through the shear modulus G and chain elongation ratio β.

To illustrate universality in nonlinear network elasticity we plotted reduced network shear modulus $G(I_1)/G$ as a function of the parameter $\beta I_1/3$ for the natural rubber, synthetic and biological networks (Figure 4). We have also included data obtained from computer simulations of the coarse-grained network model with different values of the persistence length. Remarkably, all data sets collapse into one universal line. (Note that for weakly cross-linked networks to obtain the value of the deformation dependent shear modulus we have subtracted entanglement contribution from the network stress, $\sigma_{xx}(\lambda) - \sigma^e_{xx}(\lambda)$ (see Appendix B).) The natural rubber, neurofilament networks and networks modeled in computer simulations can experience large deformations for which the extension ratio λ could be much larger than unity. These networks are made of strands with $\beta \approx \langle R_{in}^2\rangle/R_{max}^2 \ll 1$ such that there are many Kuhn segments per network strand. Note that for these networks the value of the network shear modulus is on the order of k_BT per network strand, $G(3) \equiv G \approx k_BT\rho/N_s$. The data sets for these systems occupy the region on the plot corresponding to the interval $G(I_1)/G \leq 10$ (see Table 1). The data sets covering the interval $G(I_1)/G \geq 10$ correspond to biological networks made of rigid strands (filaments) (see Table 1). For such networks, the strands between cross-links are almost fully stretched $\langle R_{in}^2\rangle \approx R_{max}^2$ ($\beta \approx 1$). The simulation data cover almost the entire interval of the strain-dependent shear modulus and support this observation.

It is important to point out that the deviation from the universal behavior takes place when the shortest strands of the network begin to support majority of the stress. Our simulations show that at such high deformations the bonds belonging to these strands begin to deform. This changes the nature of the network elasticity from

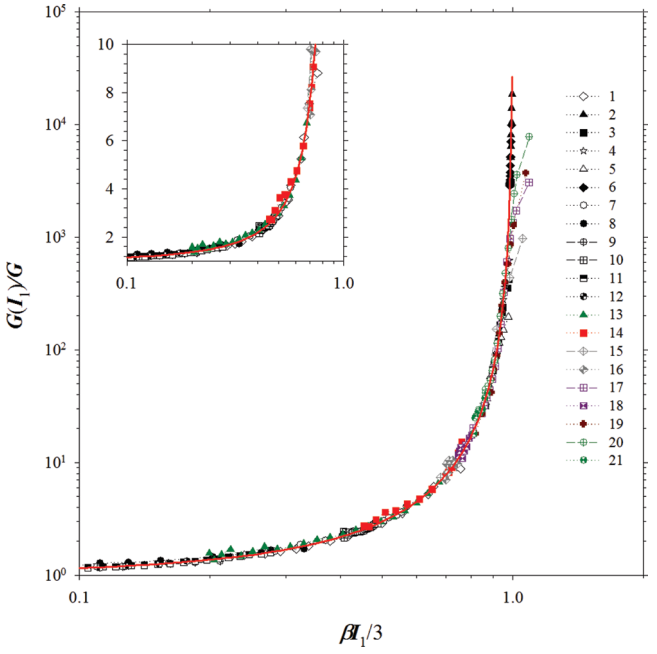

Figure 4. Dependence of the reduced strain dependent shear modulus $G(I_1)/G$ on the parameter $\beta I_1/3$. Numbers correspond to networks described in Table 1 and the solid line corresponds to eq 3.

entropic to enthalpic. Single chain stretching experiments show that a crossover to the bond stretching regime occurs when the pulling forces exceed 40−100 pN.[13,14] This onset of the local forces acting on the network strands should be considered as a crossover between the entropic and enthalpic origin of the network elasticity. Note that in the case of biological networks the crossover from entropic to enthalpic regimes in network elasticity could occur due to overstretching of the protein cross-links connecting network filaments.[22]

The uniqueness of our model of the nonlinear network elasticity is that it relates molecular parameters of the network strands with network nonlinear mechanical response. This is vital for understanding mechanical properties of rubber-like materials,[1] muscles, biological tissues,[4,23,24] cells,[25,26] and blood clots.[27] Furthermore, understanding the mechanism of the nonlinear elasticity of network and gels opens possibility for design of new materials with programmed nonlinear elastic properties. This can have a significant impact on development of synthetic substitutes for biological tissues such as skin, arterial walls, and muscles whose functions require nonlinear elastic response in a particular range of external loads.

To the end we want to comment on the crossover to the nonlinear freely jointed chain deformation regime and range of applicability of our eqs 1−3. For flexible chains this crossover occurs when external forces acting on the polymer chains are on the order of 20−300 pN. In this interval of forces the chain's end-to-end distance is about 70−90% of its fully extended length, $R/R_{\max} \approx 0.7-0.9$. Taking this into account we can estimate a value of the network elongation ratio from the following relationship, $\beta\lambda^2/3 \approx (R/R_{\max})^2 \approx 0.5-0.8$. Thus, for natural rubber samples used in the Treloar's experiments[1] the network extension ratio at the crossover to the nonlinear freely jointed chain deformation regime is on the order of $\lambda \approx 7-9$. These values are close to the largest network deformations studied by Treloar.[1] The majority of the experimental data on deformation of the polymeric networks have covered the range of the network extension ratios, $\lambda < 6$.[1] For such network deformations the deformation dependent network shear modulus can be approximated by the eqs 3a and 3b. Note that one can derive a more general expression for the network deformation by starting from expression for the chain deformation which includes the crossover to the nonlinear freely jointed chain deformation regime (see ref 18). We will consider this approach in our future publications.

Acknowledgment. This research was supported by the National Science Foundation under the grant DMR# 1004576.

Appendix A

Here we use our result for the nonlinear force-deformation relation[19] between applied force f and the average distance between chain ends $\langle R\rangle$ along the direction of the applied force for a worm-like chain with the number of bonds N

$$\frac{f}{k_B T} \approx \frac{\langle R\rangle}{\langle R_0^2\rangle} + \frac{2}{\langle R_0^2\rangle}\frac{\langle R\rangle}{(1-\langle R\rangle^2/R_{\max}^2)^2} \qquad (A.1)$$

where $R_{\max} = bN$ is a length of the fully extended chain with bond length b, $\langle R_0^2\rangle \approx 2l_p R_{\max}$ is the mean-square average end-to-end distance of an ideal chain with the persistence length equal to l_p. We assume that the chain's end-to-end distance R is equal to its average value $\langle R\rangle$ and neglect effect of fluctuations. Note that this approximation improves with increasing the chain deformation when the chain's end-to-end distance becomes on the order of its average value, $R \approx \langle R\rangle$, and the ratio of fluctuations of a chain's end-to-end distance δR to its average value is smaller than unity, $\delta R/\langle R\rangle \ll 1$. In the case of small chain deformations, $R \approx \langle R_0^2\rangle^{1/2}$ and $R/R_{max} \ll 1$, the fluctuations δR can be on the order of $\langle R_0^2\rangle^{1/2}$. In this chain deformation regime, our approximation of the eq A.1 results in an expression for the chain deformation similar to the one obtained from the Flory-like chain's elastic free energy.[5] The dependence of the chain's free energy on the chain end-to-end distance R can be obtained by using the principle of virtual work by considering eq A.1 as an equation describing force-deformation relationship of the nonlinear spring with the spring length R. The chain's free energy is calculated as a work done by stretching a chain (nonlinear spring) by a constant force f pointing along the end-to-end vector $\vec{R}$ by a distance $d\vec{R}$

$$dF = (\vec{f}\cdot d\vec{R}) \approx f(R)\, dR \qquad (A.2)$$

Performing integration over R one obtains

$$\frac{F(R)}{k_B T} \approx \frac{R^2}{2\langle R_0^2\rangle} + \frac{R_{\max}}{2l_p(1-R^2/R_{\max}^2)} \qquad (A.3)$$

Note that in the limit of the small chain deformations, $R/R_{\max} \ll 1$, eq A.3 reproduces the elastic free energy of an ideal chain.[5] Thus, our expression for the chain's free energy eq A.3 can be considered as a generalization of the Flory-like elastic free energy[5] of an ideal chain to the case of large chain deformations.

We will assume that a network is isotropic and cross-links connecting polymeric strands have in average N_s bonds each. In the framework of the affine network model[1,5] each strand deforms affinely ($R_s^x = \lambda_x R_{in}^x$, $R_s^y = \lambda_y R_{in}^y$, $R_s^z = \lambda_y R_{in}^z$) and the free energy of a network is equal to the sum of contributions from strands between cross-links.

$$F_{net}(\{\lambda_i\}) = \sum_s F(R_s) \approx GV\left(\frac{I_1(\{\lambda_i\})}{6} + \beta^{-1}\left(1-\frac{\beta I_1(\{\lambda_i\})}{3}\right)^{-1}\right) \qquad (A.4)$$

where V is the system volume, $I_1(\{\lambda_i\}) = \lambda_x^2 + \lambda_y^2 + \lambda_z^2$ is the first strain invariant of the deformation matrix, $\langle R_{in}^2\rangle$ is the mean-square average end-to-end distance of a strand between cross-links in the undeformed network, $G \approx k_B T\rho\langle R_{in}^2\rangle/\langle R_0^2\rangle N_s$ is the shear modulus of the network with monomer density ρ. $\beta = \langle R_{in}^2\rangle/R_{\max}^2$ is the ratio of the mean-square average distance

between cross-links in the undeformed network and the square of the end-to-end distance of the fully extended strand. This parameter determines how much the polymeric strands between cross-links can be stretched. In deriving expression eq A.4 we have assumed an affine deformation of the network such that $\langle R_s^2\rangle = I_1(\{\lambda_i\})\langle R_{in}^2\rangle/3$ and used a preaveraging approximation substituting $\langle(1/[1-x^2])\rangle$ by $1/(1-\langle x^2\rangle)$. Note that the accuracy of the preaveraging approximation improves when the value of the parameter $x \approx 1$ and $x \ll 1$. In the case $x \approx 1$, the fluctuations δx around the average value are small, $\delta x/\langle x\rangle \ll 1$, such that $\langle x^2\rangle \approx \langle x\rangle^2 \approx x^2$. In the opposite limit, when $x \ll 1$, we can use the following approximation $\langle 1/(1-x^2)\rangle \approx 1 + \langle x^2\rangle \approx 1/(1-\langle x^2\rangle)$. Equation A.4 is the main result of the paper. It allows us to describe elasticity of a network using two parameters: the network shear modulus G and the chain elongation ratio β.

We apply this equation to describe nonlinear stress−strain relation in a network undergoing uniaxial and shear deformations. For the uniaxial deformation at a constant volume, the product of the deformation (elongation) ratios is a constant $\lambda_x\lambda_y\lambda_z = 1$, such that the network extends in one direction while contracts in two others (see Figure 2) resulting in $\lambda_x = \lambda$; $\lambda_y = \lambda_z = 1/\sqrt{\lambda}$.[1,5] The true stress generated in the uniaxially deformed network is equal to

$$\sigma_{xx}(\lambda) = \frac{\lambda}{V}\frac{\partial F_{net}(\lambda)}{\partial\lambda} = \frac{G}{3}(\lambda^2-\lambda^{-1})\left(1+2\left(1-\frac{\beta I_1(\lambda)}{3}\right)^{-2}\right) \quad (A.5)$$

where the first strain invariant for the uniaxially deformed network is $I_1(\lambda) = (\lambda^2+2/\lambda)$. Note that for uniaxial network deformation the magnitude of the true stress is related to the engineering stress as $\sigma_{xx}^{eng} = \sigma_{xx}/\lambda$.[1,5]

For a shear the three principle extension ratios are $\lambda_1 = \lambda$; $\lambda_2 = 1/\lambda$; $\lambda_3 = 1$. It is important to point out that the direction of the principle axes of strain are not related to the direction of shear in any simple way and dependent on the magnitude of the strain. The shear strain γ is equal to $\gamma = \tan\phi = \lambda - \lambda^{-1}$[1] (see Figure 2) and the shear stress generated in the deformed network is equal to

$$\sigma_{xy}(\gamma) = \frac{1}{V}\frac{\partial F_{net}(\gamma)}{\partial\gamma} = \frac{G\gamma}{3}\left(1+2\left(1-\frac{\beta I_1(\gamma)}{3}\right)^{-2}\right) \quad (A.6)$$

where the first strain invariant for the shear deformation is given by $I_1(\gamma) = \gamma^2 + 3$.

Appendix B

The analysis of experimental data presented in Figure B1 shows that we have to modify the expression for the network free energy eq A.4 to include effect of entanglements in the range of small deformation ratios $\lambda < 2$. To account for the entanglements we added the Mooney-Rivlin term[1]

$$F_e \approx \frac{G_e V}{2}(\lambda_1^2\lambda_2^2 + \lambda_1^2\lambda_3^2 + \lambda_2^2\lambda_3^2) \quad (B.1)$$

where G_e is the contribution to the network shear modulus due to entanglements. Note that the Mooney−Rivlin term[1] is one of the possible forms of the correction term to account for the entanglement contribution. The detailed discussion of this subject can be found in refs 5 and 28 and is beyond the scope of this paper. Thus, adding this term to the network free energy eq A.4 we have for the uniaxial network deformation

$$F_{net}(\lambda) \approx GV\left(\frac{I_1(\lambda)}{6} + \beta^{-1}\left(1-\frac{\beta I_1(\lambda)}{3}\right)^{-1}\right) + \frac{G_e V}{2}\left(2\lambda + \frac{1}{\lambda^2}\right) \quad (B.2)$$

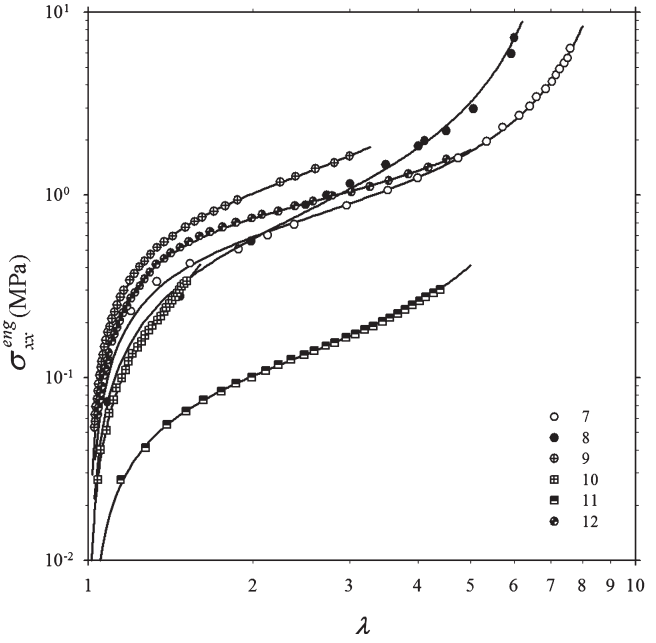

Figure B1. Dependence of the engineering stress σ_{xx}^{eng} on deformation ratio λ for polymeric networks. Numbers correspond to the networks described in Table 1, and the lines are the best fit to eq B.3.

The last expression can be considered as a generalization of the Mooney−Rivlin expression for the network free energy as a function of the first and second strain invariants. The experimental data of the uniaxial network deformation are usually report the value of the engineering stress. The engineering stress is defined as a ratio of the elongation force applied to a sample and the original cross section area of the sample. This leads to

$$\sigma_{xx}^{eng}(\lambda) = \frac{\sigma_{xx}(\lambda)}{\lambda} = \frac{G}{3}\left(\lambda-\frac{1}{\lambda^2}\right)\left(1+\frac{3G_e}{G\lambda}+2\left(1-\frac{\beta}{3}\left(\lambda^2+\frac{2}{\lambda}\right)\right)^{-2}\right) \quad (B.3)$$

We used eq B.3 to fit experimental data for uniaxial network deformation shown in Figure B1. As one can see, the agreement between the experimental data and the expression for the engineering stress is a very good. To extract from the experimental data contribution of the cross-links to the strain-dependent shear modulus $G(I_1)$ presented in Figure 4 we have subtracted from the total stress contribution from entanglements

$$G(I_1) \equiv \frac{\sigma_{xx}^{eng}(I_1)}{(\lambda-\lambda^{-2})} - \frac{G_e}{\lambda} \quad (B.4)$$

Appendix C

We have performed molecular dynamics simulations[21] of deformation of networks of semiflexible chains. Chains forming a network were modeled by bead−spring chains consisting of monomers with diameter σ. The connectivity of beads in polymer chains and the cross-link bonds were maintained by the finite extension nonlinear elastic (FENE) potential[29]

$$U_{FENE}(r) = -0.5k_sR_m^2\ln\left(1-\frac{r^2}{R_m^2}\right) \quad (C.1)$$

where k_s is the spring constant set to $k_s = 500k_BT/\sigma^2$, the maximum bond length is $R_m = 1.5\sigma$, k_B is the Boltzmann constant and T is the absolute temperature. (The large value of the spring constants was selected to minimize the effect of the

bond stretching at large network deformations). The repulsive part of the bond potential was modeled by the shifted Lennard-Jones potential with the values of the Lennard-Jones interaction parameter $\varepsilon_{LJ} = 1.5k_BT$. The chain bending rigidity was introduced into the model through a bending potential controlling the mutual orientations between two neighboring along the polymer backbone unit bond vectors $\vec{n}$ and $\vec{n}_{i+1}$

$$U_{i,i+1}^{bend} = k_B TK(1-(\vec{n}_i \cdot \vec{n}_{i+1})) \quad \text{(C.2)}$$

In our simulations the value of the bending constant K was equal to 2, 5, 10, 20, 30, and 40. For this chain model a chain persistence length l_p is related to the chain's bending constant as $l_p = b(1 + \coth(K) - K^{-1})/2(1 - \coth(K) + K^{-1})$, where $b = 0.8375 \pm 0.010\,\sigma$ is the bond length. (The system parameters are listed in Table C1). We did not have any additional interactions between monomers. This was done to maintain isotropic structure of the network and to avoid a nematic ordering of semiflexible chains.

Simulations were carried out in a constant number of particles, and temperature ensemble. The constant temperature was maintained by coupling the system to a Langevin thermostat implemented in LAMMPS.[29] In this case, the equation of motion of i^{th} bead is

$$m\frac{d\vec{v}_i(t)}{dt} = \vec{F}_i(t) - \xi\vec{v}_i(t) + \vec{F}_i^R(t) \quad \text{(C.3)}$$

where $\vec{v}_i(t)$ is the ith bead velocity, and $\vec{F}_i(t)$ is the net deterministic force acting on ith bead with mass m. $\vec{F}_i^R(t)$ is the stochastic force with zero average value $\langle \vec{F}_i^R(t)\rangle = 0$ and δ-functional correlations $\langle \vec{F}_i^R(t)\vec{F}_i^R(t')\rangle = 6\xi k_B T\delta(t-t')$. The friction coefficient ξ was set to $\xi = m/\tau_{LJ}$, where τ_{LJ} is the standard LJ-time

$$\tau_{LJ} = \sigma\sqrt{m/\varepsilon_{LJ}}$$

The velocity−Verlet algorithm with a time step $\Delta t = 0.005\tau_{LJ}$ was used for integration of the equations of motion (eq C.3). All simulations were performed using LAMMPS.[29]

The networks were prepared by starting with simulations of the 3-D periodic solutions of 96 chains with the degree of polymerizations $N = 200$ at polymer concentration $c = 0.5\sigma^{-3}$. (The initial simulation box size in all simulations was $L_0 = 33.74\sigma$). The systems were equilibrated for 10^7 integration steps. The second step involved cross-linking of polymer solutions. During this procedure neighboring monomers were randomly cross-linked by FENE bonds if they fall within 1.5σ cutoff distance from each other. One cross-link bond was allowed per monomer, thus creating a randomly cross-linked network. To minimize the polydispersity of the strands between cross-links we set the minimum number of bonds between cross-links to be $N_s = 9$. For all networks the cross-linking density was equal to $0.0125\sigma^{-3}$. After completion of the cross-linking process we have eliminated the bending potential between adjacent to the cross-link chain's bonds. Networks were relaxed by performing NVT molecular dynamics simulation runs lasting 10^7 integration steps. This was followed by a production run lasted 10^7 integration steps. During this simulation run we have obtained value of the parameter β by averaging $R_s^2/(N_s b)^2$ for each network strand between cross-links.

In order to obtain stress−strain relation for networks of semiflexible chains we have performed sets of simulations of uniaxial network deformations.[30] The networks were deformed by changing the initial box size L_0 along x direction to λL_0 and to $L_0/\sqrt{\lambda}$ in the y and z directions. Under such deformation the system volume remained the same. This deformation was achieved by a series of small affine deformations

$$\{x_i, y_i, z_i\} \rightarrow \{\Delta\lambda x_i, y_i/\sqrt{\Delta\lambda}, z_i/\sqrt{\Delta\lambda}\}$$

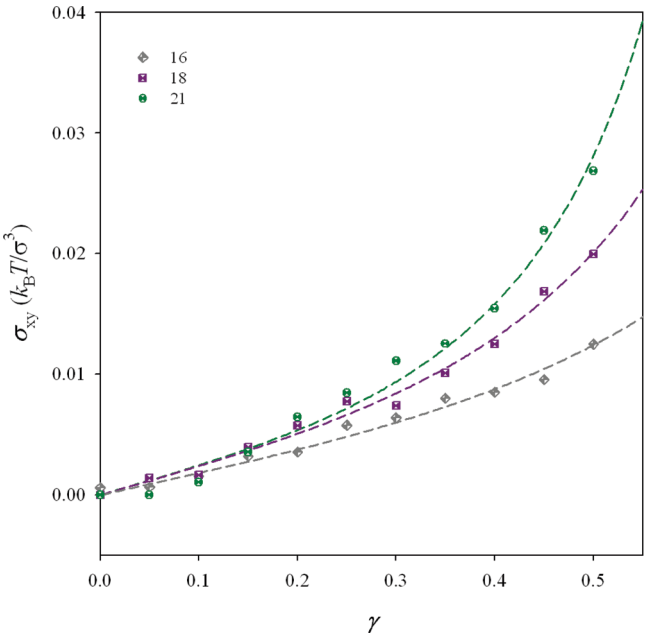

Figure C1. Dependence of the shear stress σ_{xy} on shear strain γ. Numbers correspond to networks described in Table 1.

until the desired strain was obtained. The molecular dynamics simulation proceeded during the constant-volume deformation process such that the network was allowed to adjust its conformations for 10^7 integration steps. The final 5×10^6 integration steps we used for the data averaging. The stress σ_{xx} in the direction of the strain was evaluated from the simulations through the pressure tensor P_{ij} as follows

$$\sigma_{xx} = \frac{3}{2}P_{xx} - \frac{1}{2}\sum_i P_{ii} \quad \text{(C.4)}$$

Figure 3 presents our simulation results for uniaxial network deformation.

In addition to uniaxial network deformation we have also performed simulations of networks undergoing shear deformation. The stress−strain curves for this type of the network deformation are shown in Figure C1. The lines correspond to the best fits to the following equation

$$\sigma_{xy}(\gamma) = \frac{G\gamma}{3}\left(1 + 2\left(1 - \frac{\beta}{3}(\gamma^2+3)\right)^{-2}\right) \quad \text{(C.5)}$$

Note that we only fitted the values of the chain size ratio β while the values of the shear modulus G were set to the values obtained from fitting data sets of corresponding uniaxially deformed networks.

We can use computer simulation results to test a scaling dependence of the network shear modulus on the system parameters (see Appendix A).

$$G \approx k_B T\rho\frac{\langle R_{in}^2\rangle}{\langle R_0^2\rangle N_s} \approx k_B T\rho\beta\frac{b}{b_K} \quad \text{(C.6)}$$

In simplifying the last equation we take into account that $\langle R_{in}^2\rangle \approx \beta R_{max}^2 \approx \beta b^2 N_s^2$, and $\langle R_0^2\rangle \approx b_k R_{max}$, where b_K is the Kuhn length, $b_K = 2l_p$. It follows from eq C.6 that the reduced network shear modulus $G/(k_BT\rho\beta)$ is proportional to the ratio of the bond length to the Kuhn length, b/b_K. Before proceeding further we have to point out that not all network strands support stress.[1,5] The dangling ends, connected to the network by only one end, should be excluded. The effect of the dangling ends is particularly important for networks prepared by cross-linking short polymer

Table C1. System Parameters

l_p [σ]	K [k_BT]	N_s	β_{sim}	$\beta_{fit\text{-}U}$ ($\beta_{fit\text{-}S}$)
1.391	2	17.88 ± 7.4	0.177 ± 0.130	0.198
3.771	5	18.03 ± 6.7	0.368 ± 0.181	0.450
7.956	10	17.90 ± 6.7	0.545 ± 0.175	0.633 (0.654)
16.331	20	17.98 ± 6.7	0.681 ± 0.150	0.752 (0.742)
24.706	30	17.83 ± 6.6	0.735 ± 0.141	0.791
33.081	40	17.99 ± 6.7	0.761 ± 0.144	0.806 (0.808)

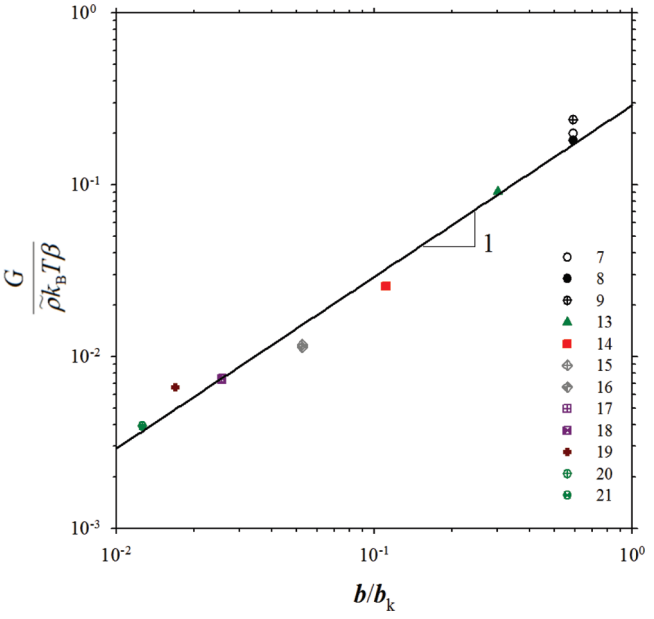

Figure C2. Dependence of the reduced shear modulus on the ratio of the bond length b to the Kuhn length b_K. Numbers correspond to networks described in Table 1.

chains. In our simulations we have prepared networks by cross-linking chains with the number of monomers $N = 200$. After cross-linking each chain has in average N/N_s network strands and two of those strands are dangling ends. Thus, the actual monomer density of the network strands that support stress is equal to

$$\tilde{\rho} \approx N_s \frac{\rho}{N}\left(\frac{N}{N_s} - 2\right) \approx \rho\left(1 - \frac{2N_s}{N}\right) \qquad \text{(C.7)}$$

The effect of the dangling ends diminishes with decreasing the ratio N_s/N.

In Figure C2, we plot the reduced network shear modulus $G/(k_BT\beta\tilde{\rho})$ as a function of b/b_K. Our simulations show that the network shear modulus decreases with increasing the chain rigidity or chain Kuhn length, $G/(k_BT\beta\tilde{\rho}) \propto b/b_K$. In addition to simulation data, we have also added to this plot data points corresponding to natural rubber. For these data, we used for the bond length $b = 0.484$ nm (this value corresponds to the total length of all four bonds of the monomeric unit of the 1,4-poly-isoprene along the chain axis in the ground state), for the Kuhn length $b_K = 0.82$ nm,[5] and for the density of the natural rubber 0.93 g/cm^3. For these networks we did not correct for the effect of the dangling ends, $\rho = \tilde{\rho}$. The simulation data are in a good agreement with experimental results for natural rubber.

References and Notes

(1) Treloar, L. R. G., *The Physics of Rubber Elasticity*; Clarendon Press: Oxford, U.K., 2005.

(2) Becker, G. W.; Kruger, O. On the nonlinear biaxial stress-strain behavior of rubberlike polymers. In *Deformation and Fracture of High Polymers*; Kausch, H. H., Hessell, J. A., Jaffee, R. I., Eds. Plenum Press: New York, 1972.

(3) Williams, S. R.; Mather, B. D.; Miller, K. M.; Long, T. E. Novel michael addition networks containing urethane hydrogen bonding. *J. Polym. Sci. A* **2007**, *45* (17), 4118–4128.

(4) Storm, C.; Pastore, J. J.; MacKintosh, F. C.; Lubensky, T. C.; Janmey, P. A. Nonlinear elasticity in biological gels. *Nature* **2005**, *435* (7039), 191–194.

(5) Rubinstein, M.; Colby, R. H. *Polymer Physics*; Oxford University Press: New York, 2003.

(6) MacKintosh, F. C. Elasticity and dynamics of cytoskeletal filaments and their networks. In *Soft condensed matter physics in molecular and cell biology*; Poon, W. C. K., Andelman, D., Eds.; Taylor & Francis: New York, 2006; pp 139−155.

(7) Kroy, K. Elasticity, dynamics and relaxation in biopolymer networks. *Curr. Opin. Colloid Interface Sci.* **2006**, *11* (1), 56–64.

(8) Heussinger, C.; Schaefer, B.; Frey, E. Nonaffine rubber elasticity for stiff polymer networks. *Phys. Rev. E* **2007**, *76* (3), 031906.

(9) Conti, E.; MacKintosh, F. C. Cross-Linked Networks of Stiff Filaments Exhibit Negative Normal Stress. *Phys. Rev. Lett.* **2009**, *102* (8), 088102.

(10) Onck, P. R.; Koeman, T.; van Dillen, T.; van der Giessen, E. Alternative explanation of stiffening in cross-linked semiflexible networks. *Phys. Rev. Lett.* **2005**, *95* (17), 178102.

(11) Marko, J. F.; Siggia, E. D. Stretching DNA. *Macromolecules* **1995**, *28* (26), 8759–8770.

(12) Smit, S. B.; Cui, Y. J.; Bustamante, C. Overstretching B-DNA: The elastic response of individual double-stranded and single-stranded DNA molecules. *Science* **1996**, *271*, 795–799.

(13) Bustamante, C.; Smith, S. B.; Liphardt, J.; Smith, D. Single-molecule studies of DNA mechanics. *Curr. Opin. Struct. Biol.* **2000**, *10* (3), 279–285.

(14) Williams, M. C.; Rouzina, I. Force spectroscopy of single DNA and RNA molecules. *Curr. Opin. Struct. Biol.* **2002**, *12* (3), 330–336.

(15) Toan, N. M.; Thirumalai, D. Theory of biopolymer stretching at high force. *Macromolecules* **2010**, *43*, 4394–4400.

(16) Rosa, A.; Hoang, T. X.; Marenduzzo, D.; Maritan, A. Elasticity of semiflexible polymers with and without self-interactions. *Macromolecules* **2003**, *36*, 10095–10102.

(17) Livadaru, L.; Netz, R. R.; Kreuzer, H. J. Stretching response of discrete semiflexible polymers. *Macromolecules* **2003**, *36*, 3732–3744.

(18) Dobrynin, A. V.; Carrillo, J.-M. Y.; Rubinstein, M. Chains are more flexible under tension. *Macromolecules* **2010**, *43*, 9181–9190.

(19) Carrillo, J.-M. Y.; Dobrynin, A. V. Effect of the electrostatic interactions on stretching of semiflexible and biological polyelectrolytes. *Macromolecules* **2010**, *43*, 2589–2604.

(20) Pechhold, W. Deformation of polymers as explained by the meander model. In *Deformation and Fracture of High Polymers*; Kausch, H. H., Hessell, J. A., Jaffee, R. I., Eds.; Plenum: New York, 1972; pp 301−315.

(21) Frenkel, D.; Smit, B., *Understanding Molecular Simulations*; Academic Press: New York, 2002.

(22) Kasza, K. E.; Koenderink, G. H.; Lin, Y. C.; Broedersz, C. P.; Messner, W.; Nakamura, F.; Stossel, T. P.; MacKintosh, F. C.; Weitz, D. A. Nonlinear elasticity of stiff biopolymers connected by flexible linkers. *Phys. Rev. E* **2009**, *79*, 041928.

(23) Janmey, P. A.; McCormick, M. E.; Rammensee, S.; Leight, J. L.; Georges, P. C.; Mackintosh, F. C. Negative normal stress in semiflexible biopolymer gels. *Nat. Mater.* **2007**, *6* (1), 48–51.

(24) Kang, H.; Wen, Q.; Janmey, P. A.; Tang, J. X.; Conti, E.; MacKintosh, F. C. Nonlinear Elasticity of Stiff Filament Networks: Strain Stiffening, Negative Normal Stress, and Filament Alignment in Fibrin Gels *J. Phys. Chem. B* **2009**, *113* (12), 3799–3805.

(25) Gardel, M. L.; Kasza, K. E.; Brangwynne, C. P.; Liu, J. Y.; Weitz, D. A. Mechanical Response of Cytoskeletal Networks. In *Biophysical Tools for Biologists, Vol. 2: In Vivo Techniques*; 2008; Vol. *89*, p 487.

(26) Kasza, K. E.; Rowat, A. C.; Liu, J. Y.; Angelini, T. E.; Brangwynne, C. P.; Koenderink, G. H.; Weitz, D. A. The cell as a material *Curr. Opin. Cell Biol.* **2007**, *19* (1), 101–107.

(27) Weisel, J. W. Biophysics - Enigmas of blood clot elasticity. *Science* **2008**, *320* (5875), 456–457.

(28) Rubinstein, M.; Panyukov, S. Elasticity of polymer networks. *Macromolecules* **2002**, *35*, 6670–6686.

(29) Plimpton, S. J. Fast parallel algorithms for short-range molecular dynamics. *J. Comput. Phys.* **1995**, *117*, 1–19; lammps.sandia.gov .

(30) Grest, G. S.; Putz, M.; Everaers, R.; Kremer, K. Stress-strain relation of entangled polymer networks. *J. Non-Cryst. Solids* **2000**, *274* (1−3), 139–146.